Numerical analysis of multiple phase change materials based heat sink with angled thermal conductivity enhancer

Nedumaran, Muthamil Selvan; Nagarajan, Gnanasekaran; Hooman, Kamel

DOI
10.1016/j.est.2022.105316

Publication date
2022

Document Version
Final published version

Published in
Journal of Energy Storage

Journal of Energy Storage 55 (2022) 105316

Contents lists available at ScienceDirect

Journal of Energy Storage

journal homepage: www.elsevier.com/locate/est

Research papers

Numerical analysis of multiple phase change materials based heat sink with angled thermal conductivity enhancer

Muthamil Selvan Nedumaran [a], Gnanasekaran Nagarajan [a], Kamel Hooman [b,*]

[a] Dept. of Mechanical Engineering, National Institute of Technology Karnataka, Surathkal 575025, India
[b] Dept. of Process and Energy, Delft University of Technology, 2628 CB Delft, Netherlands

ARTICLE INFO

Keywords:
Electronic cooling
Triple PCM design
Melting
Tilted fin heat sink
Enthalpy porosity technique

ABSTRACT

Phase change materials (PCM) RT-28HC, RT-35HC, and RT-44HC with three different melting temperatures, 29 °C, 36 °C, and 44 °C, with similar thermal properties, are considered. The PCM is oriented from the left to right side of the heat sink in its increasing order. The fins are attached to the heat sink longitudinally, and its orientation effects are studied low (100–500 W/m^2) and high (1000–5000 W/m^2) heat fluxes applied on the horizontal bottom surface of the heat sink. A 2D model is developed using ANSYS Fluent 19, and the fin orientation effects are investigated numerically. The orientation of fins at different angles such as 0°, +15°, +30°, +45°, +60°,-15°,-30°,-45°, −60° are considered. The effect of fins on the charging cycle is assessed by comparing a single and double PCM heat sink. Three initial conditions are investigated by altering the initial temperature 300 K, 303 K, and 310 K. At increasing heat input, the negative angled fins possess a higher melting rate. For different initial conditions, −60° provides higher enhancement, and +60° possesses prolonged melting for almost all cases. The performance of a triple PCM design is compared with single and double PCM counterparts under similar conditions.

1. Introduction

Thermal management is essential for the maximum performance of devices. If the heat generated increases inside the device, the possibility of failure rises and the lifetime diminishes. Fans are used for high-end power devices to provide the desired cooling for longer usage. However, in low-end devices (portable), a fan may increase the size and weight which is not preferable. So, an alternative cooling method is a passive technique like the inclusion of phase change material (PCM). Currently, PCM is employed in various applications as a cooling medium, and its significance is explored. PCM is incorporated in the rooftops [1] and sandwiched between walls [2] to maintain thermal comfort. In solar PV, increments in power generation and temperature control in a module are achieved by PCM storage [3,4]. Concentrated solar power plant (CSP) heavily relies on thermal storage, and PCM is a very popular option for high-temperature heat storage [5–7]. PCM is employed in batteries to maintain efficient conditions and increase the service life [8,9]. In air-conditioning, with a focus on minimizing energy consumption, PCM is integrated with air conditioning systems in buildings [10] and transportation [11].

PCM is widely used for its high energy density, cycling stability, and chemical stability. PCM should be selected based on the operating temperature. Their wide range of availability for different required temperatures make them an excellent pick for a thermal control unit. Despite its various advantages, PCM has a major barrier: poor thermal conductivity. Because of its low thermal conductivity, it is not implemented in most active device applications. To increase its thermal conductance, several researchers have come across different approaches. Joseph and Sajith [12] mixed graphene fillers with PCM to improve thermal conductivity. The addition of nanoparticles with uniform and periodic heat input, including forced convection was discussed. Their study found an 11–23 % enhancement in energy savings for a hybrid heat sink. Du et al. [13] numerically approached the addition of copper nanoparticles to paraffin to enhance effective conductivity. They observed that the melting rate was increased and saved 19.6 % of melting time compared with pure PCM-based heat sink. The inclusion of copper nanoparticles attenuated non-uniformity. The effect of adding graphite particle fillers was evaluated by Srinivasan et al. [14]. As a result of filler usage, the thermal conductivity and viscosity have been drastically improved. A 3.5 % volume of additives increases thermal conductivity by 450 %. Likewise, in a storage system PCM was microencapsulated to improve the heat transfer. Gao et al. [15] established a one-dimensional numerical approach to simulate packed bed

* Corresponding author.
E-mail address: k.hooman@tudelft.nl (K. Hooman).

https://doi.org/10.1016/j.est.2022.105316
Received 29 October 2021; Received in revised form 5 July 2022; Accepted 12 July 2022
Available online 8 August 2022

Nomenclature

A	mushy zone constant
b	width (mm)
c_p	specific heat (kJ/kg.K)
$\vec{g}$	acceleration due to gravity (m/s^2)
H	enthalpy (J/kg)
h	height (mm)
h_s	sensible enthalpy (J/kg)
k	thermal conductivity (W/mK)
L	latent heat of fusion (kJ/kg)
l	length (mm)
P	pressure (N/m^2)
PCM	phase change material
q	heat flux (W/m^2)
SPT	setpoint temperature
T	temperature (K)
t	time (s)
T_l	liquidus temperature
T_m	melting temperature of PCM
T_s	solidus temperature
$\vec{v}$	velocity field (m/s)
w	thickness (mm)

Greek symbols

ρ	density (kg/m^3)
μ	dynamic viscosity (kg/ms)
β_0	coefficient of thermal expansion(1/K)
Φ	liquid fraction
λ	constant
θ	orientation angle

Subscripts

f	fin
p	PCM
s	sink
st	substrate
θ_i	fin orientation of respective cases for the initial condition
st_i	straight fin case for the initial condition

PCM storage. They found that reducing the capsule diameter can positively affect the storage unit, i.e., the effective heat storage time was shortened by 20 % because of encapsulation. PCM was micro-encapsulated and investigated numerically by Su et al. [16] to reduce the indoor temperature. Laminated binary encapsulated PCM provides better thermal performance than other types of walls. A binary encapsulated wall reduced the peak indoor air temperature by 2.9–6.7 °C.

Other than the inclusion of external particles to PCM, the addition of fins, heat pipes, and insertion of foams that can act as heat spreaders were also explored by authors. Mahmoud et al. [17] conducted experiments for various configurations of machined fins. The heat sink melting rate is shortened when increasing the number of fins. The inclusion of PCM with lower melting points for a longer period provides lower operating heat sink temperature. Marri et al. [18] developed a cylindrical heat sink with radial plate fins. In their study, the effects of ambient temperature and phase change on heat sinks were considered. Based on the increase in ambient temperature from 20 °C to 28 °C, the time to reach set point temperature is reduced by 2.3 times. The addition of angled fins to enhance the melting rate was proposed by Ji et al. [19]. The melting rate was increased by the orientation of the fin towards the bottom, resulting in uniform melting. The non-uniform melting within the PCM was surpassed by inserting tilted fins. Yang et al. [20] tested the effect of aspect ratio and tilt angle of the tank. In small aspect ratio cases, when the heating surface is placed in the horizontal position, the PCM melted fast, and in the vertical position, melting was slow. In the case of a larger aspect ratio, the melting was faster when the heating surface was inclined. In all the inclination angle cases, the heat conduction capability was the same, but the difference in melting rate was due to the natural convection. A triplex tube heat exchanger with fins for simultaneous charging and discharging was investigated by Mahdi et al. [21]. Their numerical study includes the optimization of fin structure and that optimum fin structure has a significant effect over the heat storage. Further addition of Al_2O_3 shows only a slighter improvement in melting rate.

Additionally, the authors also discussed the effect of fin configuration, fin density, fin length, and fin spacing. Desai et al. [22] analyzed the effect of fin geometry, the number of fins, and the volume of fins to control the peak temperature in electronic devices. The fin number increases from 1 to 100, and a minimum peak temperature value is observed at 100 fins. The inverted fin geometry provides a high surface area and increases heat dissipation. The inverted prism configuration with a 20 % mass of fins provides the lowest peak temperature. Ji et al. [23] investigated the effect of double-fin length in a PCM storage unit. The fin is placed internally on the vertical sidewalls, and the effect of fin length variation on the liquid fraction is noted. The results reveal that the shorter upper fin and longer lower fin accelerates the melting by high heat absorption. A total melting time of 25 % was saved when considering the fin ratio as 0.25. Arshad et al. [24] presented a 2D numerical model for the thermal management of electronic units. The fin volume fraction is varied by 10 % and 20 %, and the fin height is varied by 10 mm, 15 mm, and 20 mm. The inclusion of fins reduces the base temperature by extracting heat from the base to the ambient. The lower temperature of the heat sink was observed in the heat sink with a higher volume fraction and fin height. During the charging/discharging cycles, the effect of fin spacing, fin volume, and cavity orientation was studied by Kasper et al. [25]. An optimal fin ratio of 10–15 % with fin spacing of 25 mm provides a faster charging rate and storage capacity. On different orientations with lesser fin spacing, the heat absorption is higher, and the melting/solidification time is reduced.

Mahdi and Nsofor [26] employed multiple segment metal foam and also discussed the effect of different heat sink arrangements. Non-uniformity of temperature distribution is suppressed by cascading of metal foams in the heat sink. Partial filling of metal foam was investigated experimentally by Zhu et al. [27]. An operating temperature of 100 °C is considered as a critical time for protecting the heat sink. At lower heating power, pore size has a negligible effect on the protection time. With an increase in filling height, the effectiveness of the heat sink falls at lower heating power. Whereas for higher heating power, 2/3 partial filling has higher effectiveness. Similarly, Zhao et al. [28] studied the effect on PCM-based heat sink using a partial filling of metal foams. Their results show that fully filled foams with higher porosity are preferred for an effective heat sink with a fixed volume of foams. Dinesh and Bhattacharya [29] developed a numerical model to study the effect of pore size in a heat sink. The complete melting period was shorter for smaller pore radius for both high and low porosity values. Lower porosity for similar pore size provides higher energy absorption in a heat sink. An experimental study of the melting behavior of PCM was presented by Zheng et al. [30]. They also included a copper foam to study the effect of heating position on the melting rate. The addition of copper foams reduces the thermal resistance and reduces the melting time by 20.5 % compared with pure PCM. Natural convection diminishes with the addition of foams inside the heat sink. Similar to the previous author, the experimental observation of Mancin et al. [31] for a basal heating foam-filled storage tank shows similar results. Furthermore, in their

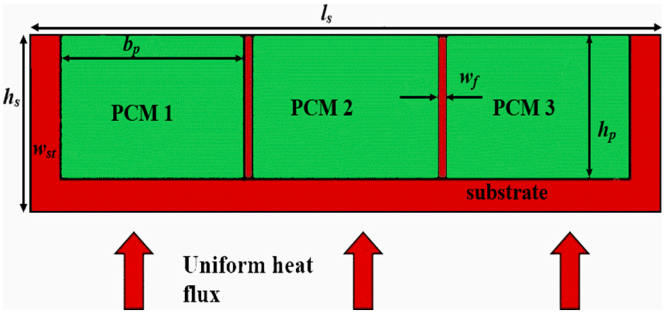

Fig. 1. 2-D Geometry of multiple PCM-based heat sinks.

study, the presence of metal foam lowers the surface temperature compared with the no-foam case.

Instead of adding external materials or fins to the heat sink, different PCMs were inserted into a single system to enhance the charging and discharging processes. Cheng and Zhai [32] developed a three-stage cascaded cold storage unit. The storage unit is filled with three different PCMs. Their observations show that exergy efficiency is higher for a three-stage cascaded cold storage unit. A brief analysis of multiple PCMs incorporated into the storage system was presented by Narasimhan [33]. According to his review, multiple PCMs yield faster charging and discharging rates than a single PCM, and also uniform exit temperature is noticed with multiple PCM storage units for a heat exchanger. Thermodynamic irreversibilities can be minimized by employing multiple PCMs. Elsanusi and Nsofor [34] evaluated the melting process of a storage unit with multiple PCMs. The authors compared series and parallel arrangements and noted that the former provides a faster melting rate. The multiple PCM arrangements also increase the energy storage capacity by 25 %. Incorporating multiple PCMs in a solar still to increase the productivity was investigated by Vigneswaran et al. [35]. It was observed that multiple PCM-based solar still produces higher yield while their efficiency is favorably higher. The yield for multiple PCM compared with single PCM and no fin was found to be 19 % and 9.5 % higher. Ezra et al. [36] numerically analyzed a multiple PCM incorporated in a storage unit. In the mathematical model, sensible heat capacities of tubes and molten PCM were also considered, which leads to comprehensive relations. Those relations provide an optimal configuration for any number of materials and their melting temperature span, leading to shorter melting. Mahdi et al. [37]

Table 1
Properties of the materials.

Thermal Properties		Unit	RT-28HC [45,46]	RT-35HC [46,47]	RT-44HC [46,48]	Aluminum [49]
Density ρ		kg/m^3	770	778.2	700	2719
Specific heat c_p		kJ/kg.K	2	2	2.1	0.871
Heat of fusion L_p		kJ/kg	241	220	218	–
Thermal conductivity k		W/m.K	0.2	0.116	0.2	202.4
Dynamic viscosity μ		kg/m.s	0.002387	0.0044	0.008	–
Thermal expansion coefficient β_0		K^{-1}	0.0005	0.000865	0.00259	–
Phase change temperature	T_s	K	300.15	307.65	315.5	–
	T_l		302.15	309.15	317.15	–

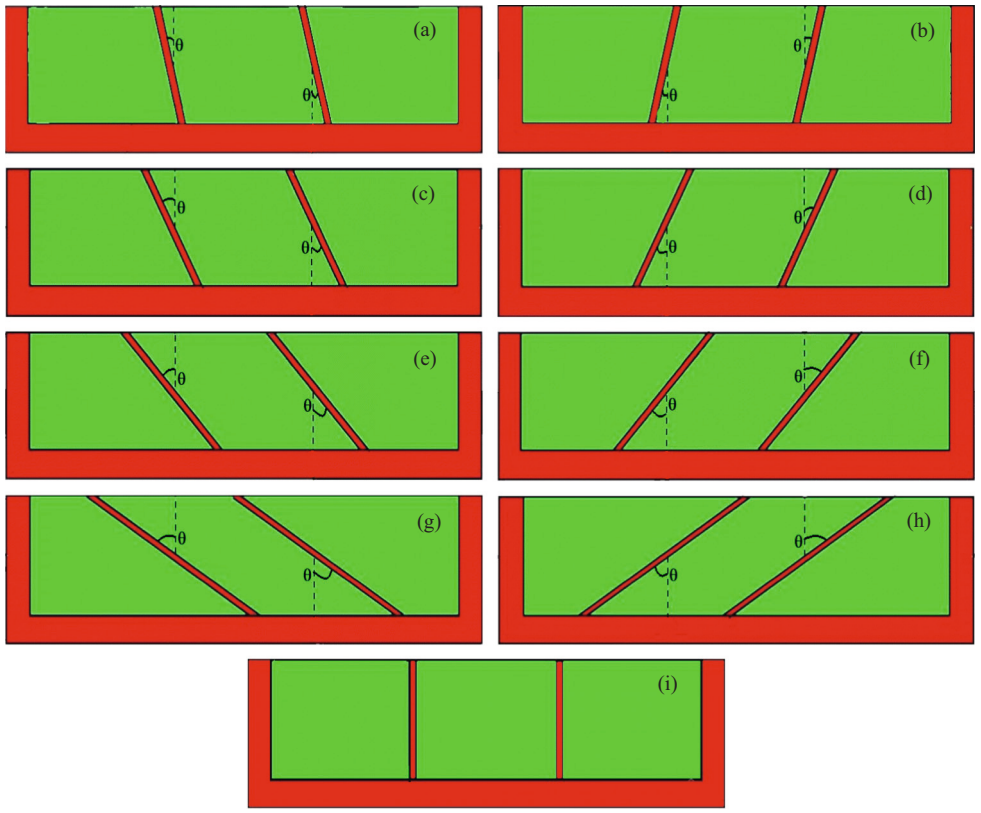

Fig. 2. Design of tilted fins with various angles: (a) +15° (b) -15° (c) +30° (d) -30° I + 45° (f) -45° (g) +60° (h) -60° (i) 0°.

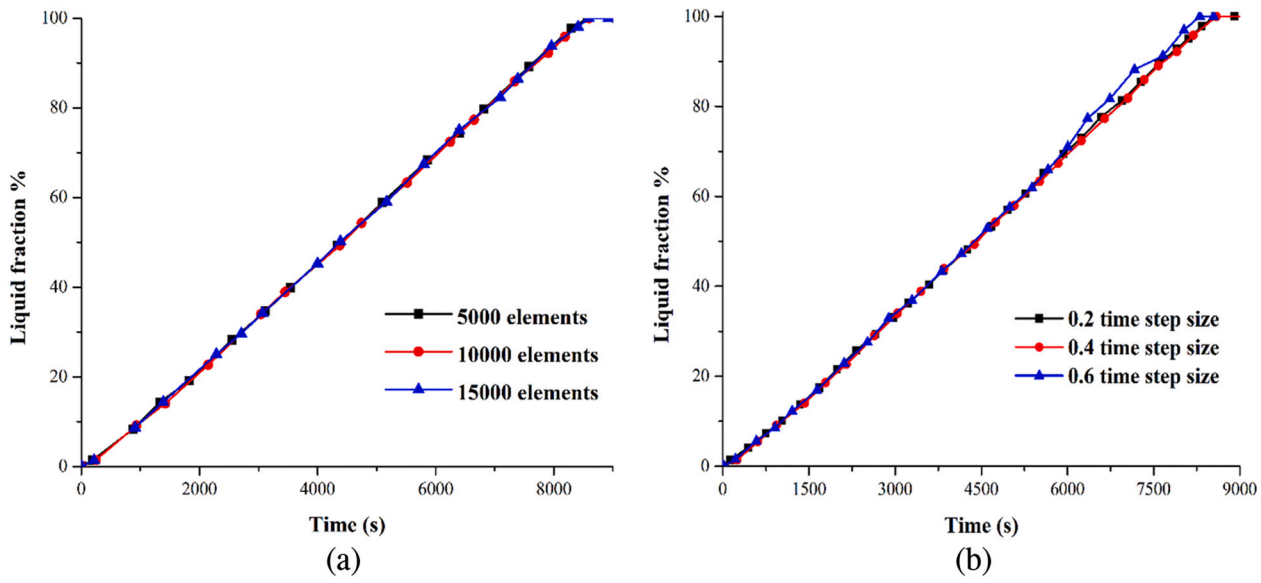

Fig. 3. Grid independence study.

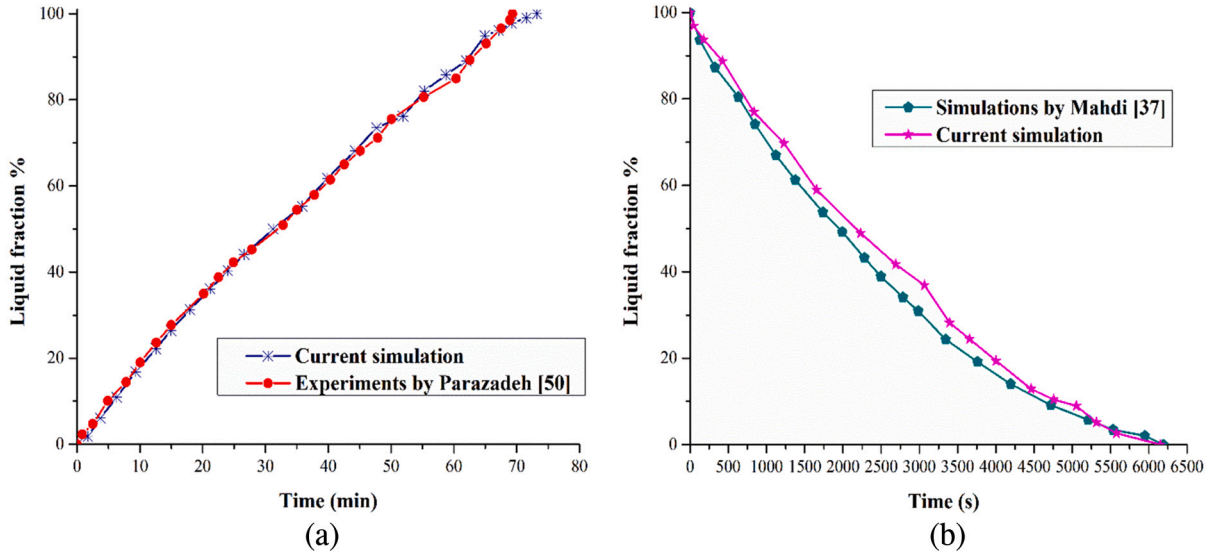

Fig. 4. Validation for (a) single PCM and (b) multiple PCM.

Table 2
Different arrangements of multiple PCM.

Cases	PCM-1	PCM-2	PCM-3
A	RT-44HC	RT-28HC	RT-35HC
B	RT-44HC	RT-35HC	RT-28HC
C	RT-35HC	RT-44HC	RT-28HC
D	RT-35HC	RT-28HC	RT-44HC
E	RT-28HC	RT-35HC	RT-44HC
F	RT-28HC	RT-44HC	RT-35HC

investigated the solidification of PCM in different arrangements. The hybrid system consists of only multiple PCM, multiple PCM with metal nanoparticles, and multiple PCM with cascaded metal foams. Uniform temperature distribution is found with an increasing number of PCM layers. A hybrid system consisting of metal foam and multiple PCM shows higher discharging rate which is 17 times faster when compared with other cases.

Several studies exhibit an inclusion of PCM integrated with the thermal spreader in an electronic device, reducing the thermal resistance within the system and regulating the operating temperature. Usman et al. [38] considered the staggered and in-line arrangement of PCMs for cooling electronics. Pin-fin was integrated with different types of PCMs to enhance the melting rate. Their studies indicate that triangular in-line configuration leads to elongated latent heat and shortened latent cooling phases. A composite PCM heat sink was designed to analyze the effect of different parameters on a heat sink, and guidelines were established [39]. The PCM should be selected from the guidelines to maximize the storage potential, and PCM should allow heat to be easily absorbed or released. Next, the PCM melting temperature should permit complete phase change conversion. Hayat et al. [40] developed a hybrid system with heat pipe and porous material inside a PCM-based heat sink for low-end electronics. Integration of these enhancers into PCM reduces the base temperature by delaying the phase change of PCM. If supercooling is found in the PCM, it can be reduced by the high conducting foams and heat pipes. A 2-D numerical model was developed by Arshad et al. [41] to investigate the performance of finned PCM heat sinks. The thickness of the fin is varied, and uniform heat distribution

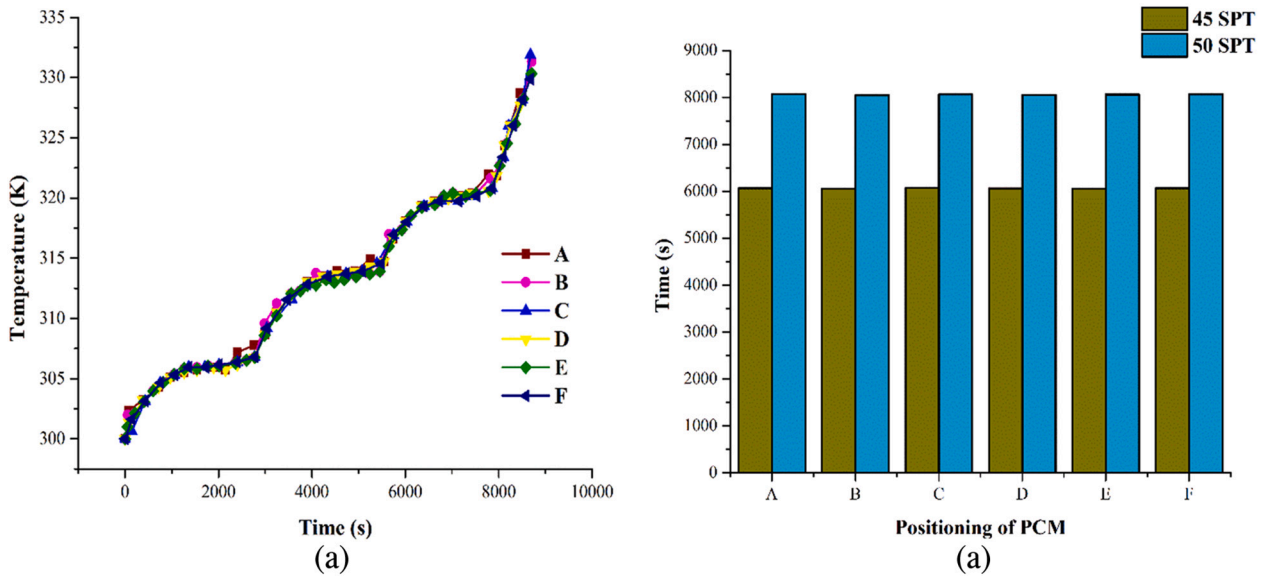

Fig. 5. (a) Heater temperature v/s time. (b) Time to attain setpoint temperature for different positioning of PCM.

was observed between the fins. Among 2 mm and 3 mm fin thickness, 3 mm has a better thermal outcome to stable the base temperature of the heat sink and lower the maximum operating temperature. A new correlation between liquid fraction and Nusselt number has been established. Sahoo et al. [42] assessed the importance of PCM-based heat sink for electronic cooling. Their literature review briefly discussed PCM with nanoparticles and the performance of metal foams on a heat sink. Their study comprised the heat sink under uniform and transient heat loads. The high amount of PCM reduces the base temperature and the amplitude of temperature fluctuation during cyclic loading at high heat flux. Leong et al. [43] developed a cross fin structured heat sink to provide an efficient system that operates at optimum temperature. According to their analysis, the base temperature of the heat sink reduced as the fin increased. The lower base temperature attained for the cross-fin heat sink was found to be 46.9 °C. The selection of PCM also influences the system.

From the above research, it is noted that incorporating multiple PCM can impact heat transfer performance. It also helps in maintaining the heat sink temperature below the critical temperature. Moreover, the application of multiple PCMs for electronic cooling is yet to be thoroughly investigated in the literature. An extended melting time of PCM based heat sink can store energy for a longer period. Thus absorbs the thermal stress offered by the device for a prolonged time and increases the lifetime of the device. This study aims to present a numerical study for a prolonged charging cycle with a multiple PCM storage heat sink. A combination of two types of enhancers comprises a hybrid heat sink to provide a required outcome. In this work, a hybrid system, with fins as thermal spreaders, is introduced to the multiple PCM storage units. Generally, the chosen material does not have similar thermal properties for different melting temperatures. Here, nonetheless, three different PCMs, RT-28HC, RT-35HC, and RT-44HC, with almost identical thermophysical properties, are taken into consideration. The objective is to characterize the effect of fin orientation for prolonged melting and also to assess the significance of a triple PCMs system during melting compared to single and double PCM designs. The initial conditions of the sink and PCM are varied, and their significance is also analyzed. The melt fraction, temperature distribution, and enhancement percentage are explored for various heat fluxes.

2. Problem description

2.1. Geometry model

Compared to the 2D model, the 3D model provides a better understanding of melting behavior within PCM. But the computational time for a 3D model is usually very high than a 2D model. The 3D model requires a large computational run to design a practical storage system. From author [44], it is clear that melt fraction of 2D is very reliable for the melting process. Hence, the numerical model can be simplified to a 2D model. When the extension is towards the z-direction, the natural convection also influences the melting. In the 3D model, once melting starts, the sink of the solid PCM to the bottom surface will be bi-directional. Whereas for 2D, the solid sunk motion is uni-directional. So, the natural convection will increase the performance for the 3D case, and the melting rate will be accelerated.

By utilizing a two-dimensional model, the numerical solution of PCM-based heat sinks can be simplified, as depicted in Fig. 1. A rectangular cavity made of aluminum contains the PCM cavity and acts as a thermal spreader. The dimensions of the rectangular cavity are l_s (100 mm), h_s (25 mm), and w_{st} (5 mm). Heat input is specified by uniform heat flux (q) and is defined at the bottom of the heat sink. Three different PCM are placed inside the aluminum sink, with equal b_p (29 mm) and h_p (20 mm) dimensions. RT-28HC, RT-35HC, and RT-44HC are the materials employed, and these are arranged in the increasing order of their melting temperature, respectively. In order to restrict the heat sink temperature below 48 °C, these materials are selected with melting temperatures ranging between 28 °C to 44 °C. Properties of the materials incorporated are listed in Table 1.

Among the PCMs, two fins with a thickness (w_f) of 1.5 mm each are placed between them to provide uniform cooling. These fins can act as a thermal spreader and a splitter to contain different materials. For a favorable thermal performance, fins with equal thickness are oriented at different angles. By placing the vertical fin as a reference, the inclination angle (θ) ranges from positive orientation, 60° (left side of vertical fin) to negative orientation, −60° (right side of vertical fin). Aluminum is selected as a material for both substrate and fins. Fig. 2 projects the geometry of 9 different cases included in this study.

2.2. Governing equations

A transient formulation with a constant thermophysical property for

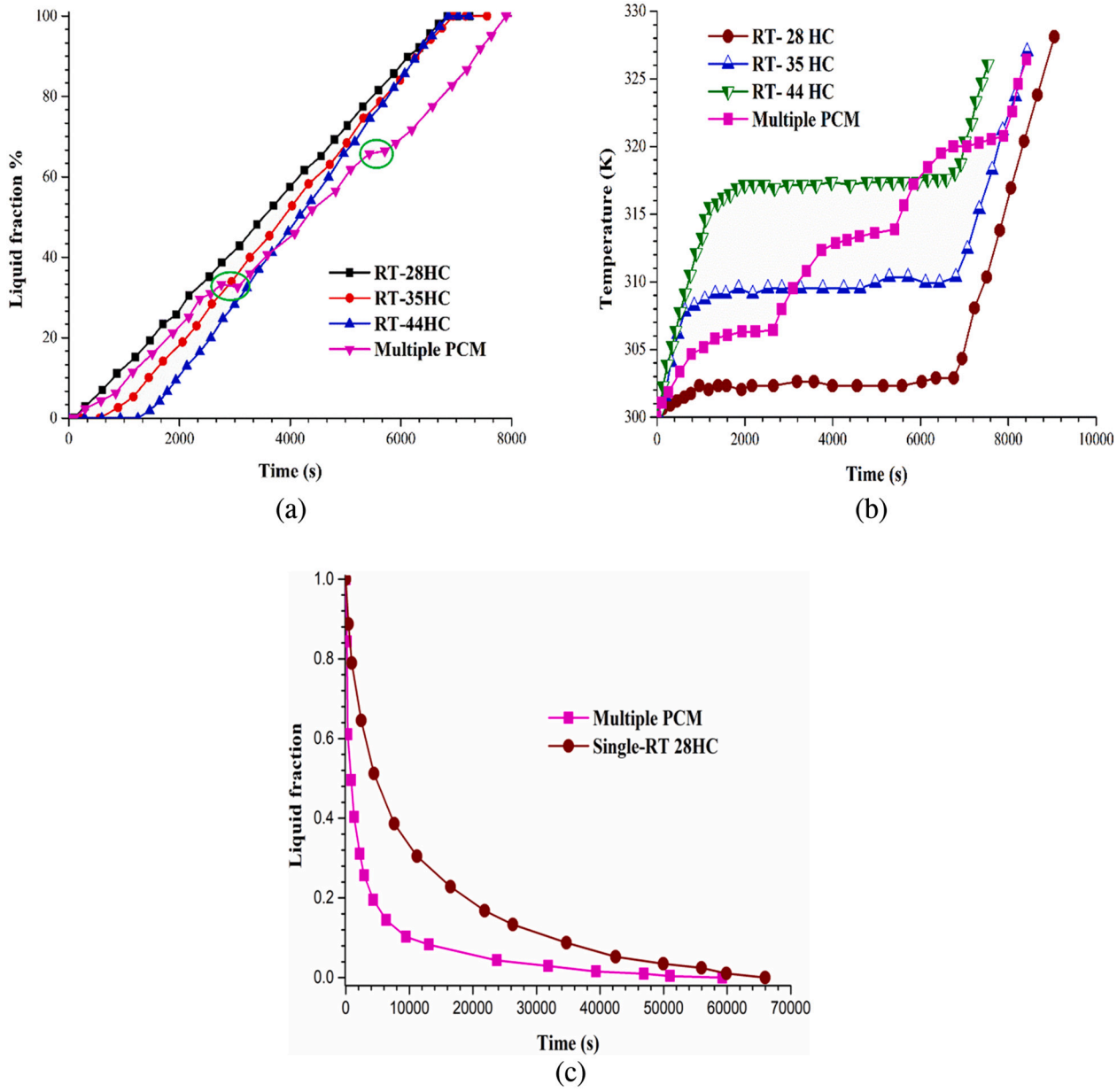

Fig. 6. Comparison of single PCM v/s multiple PCM (a) Liquid fraction v/s time (b) Heater temperature v/s time and (c) Solid fraction v/s time.

Table 3
Different cases of double PCM filled heat sink.

Cases	PCM-1	PCM-2	PCM-3
A'	RT-35HC	RT-28HC	RT-35HC
B′	RT-44HC	RT-28HC	RT-44HC
C′	RT-28HC	RT-35HC	RT-28HC
D′	RT-44HC	RT-35HC	RT-44HC
E'	RT-28HC	RT-44HC	RT-28HC
F′	RT-35HC	RT-44HC	RT-35HC

PCM (except for density) and laminar flow is considered. The fluid is assumed to be Newtonian and incompressible. During the charging cycle, the expansion of PCM is neglected. Natural convection can be exploited by applying the Boussinesq approximation within the PCM. An enthalpy-based formulation is adopted in this work, where the liquid fraction is not tracked explicitly. The governing equations with the assumptions above [49] are,

Continuity and Momentum equations:

$$\frac{\partial \rho_p}{\partial t}+\frac{\partial(\rho_p u)}{\partial x}+\frac{\partial(\rho_p v)}{\partial y}=0 \tag{1}$$

$$\rho_p \frac{D\vec{v}}{Dt}=\mu\nabla^2\vec{v}-\nabla P+\rho_p\beta_0(T_m-T)\,\vec{g}+A\,\frac{(1-\Phi)^2}{(\Phi^3+\lambda)}\vec{v} \tag{2}$$

Energy equation:

$$\frac{\partial}{\partial t}(\rho H)+\nabla\bullet(\rho\vec{v}H)=\nabla\bullet(k\nabla T) \tag{3}$$

$$\Phi=0, if\ T<T_s \tag{4}$$

$$\Phi=1, if\ T>T_l \tag{5}$$

$$\Phi=\frac{T-T_s}{T_l-T_s}\ if\ T_s<T<T_l \tag{6}$$

The thermal expansion coefficient (β_0) and density (ρ_p) of PCM are

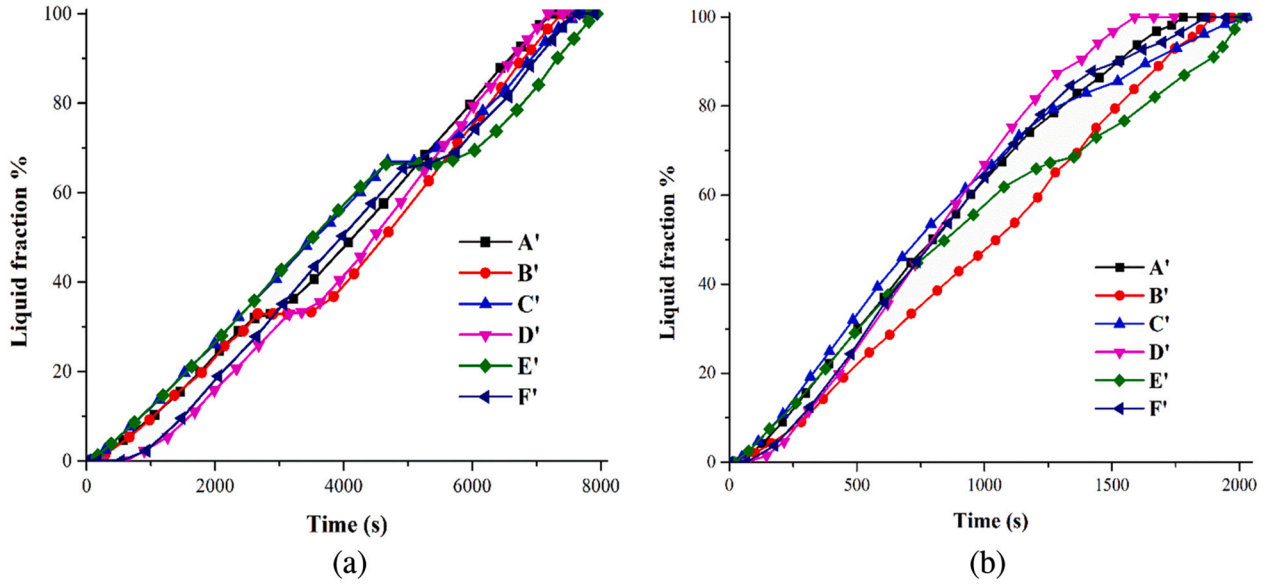

Fig. 7. Liquid fraction percentage of double PCM heat sink (a) For 500 W/m^2 and (b) 3000 W/m^2.

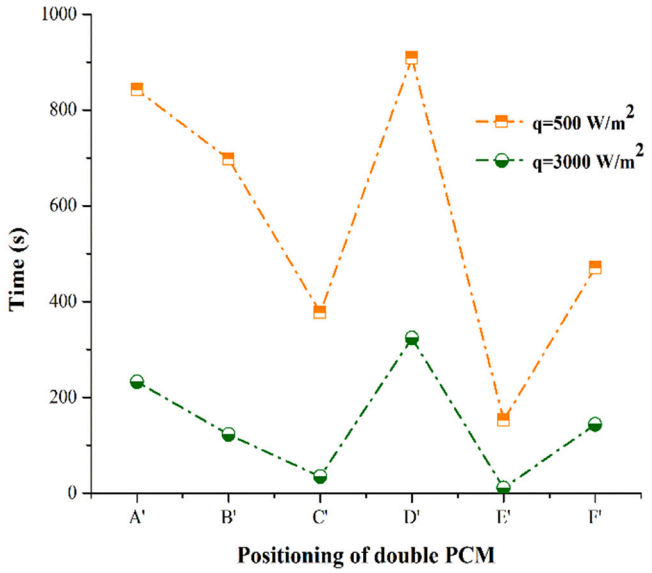

Fig. 8. Time difference between double PCM and multiple PCM for completion of charging cycle.

accounted for in their liquid state. Acceleration due to gravity ($\vec{g}$) is used to account for natural convection in the momentum equation. The liquid fraction (Φ) varies from 0 to 1, where 0 and 1 are the solid and liquid states of PCM, respectively. It is calculated from Eqs. (4)–(6). A mushy zone is a region between the solid and liquid phases during its phase change. This mushy zone is accounted for in the momentum equation as the last source term on the right-hand side of Eq. (2), where A is the mushy zone constant that ranges from 10^4 to 10^7. λ assumes a small value (here 0.001) to avoid dividing by zero.

$$H = h_s + \Phi L_p \tag{7}$$

$$h_s = h_{ref} + \int_{T_r}^{T} c_p \mathrm{d}T \tag{8}$$

In Eq. (3), H is the enthalpy comprising both sensible and latent enthalpy. The sensible and latent enthalpy are computed from Eq. (7) and Eq. (8). Where T_r is the reference temperature and h_{ref} is reference enthalpy at T_{ref}. L_p is the heat of fusion of PCM.

2.3. Numerical details

Different grid sizes such as 5000, 10,000, and 20,000 elements with a constant time step size of 0.4 s are simulated, and liquid fraction vs. time is plotted in Fig. 3. For heat flux of 400 W/m^2, the time step sizes of 0.2, 0.4, and 0.6 were tested by fixing 10,000 elements, and the liquid fraction results are plotted. After the comparison, the grid size and time step size selected for the simulation are 10,000 elements and 0.4 s step size.

A finite volume method (FVM) technique-based commercial software ANSYS Fluent 19 is applied to solve the governing equations. The SIMPLE algorithm and PRESTO scheme are employed for the pressure-velocity coupling and pressure correction equation. The second-order upwind scheme has been opted for the discretization of momentum and energy equations. The convergence criterion considered for continuity, momentum, and energy equation is 10^{-5}, 10^{-5}, and 10^{-8}, respectively.

2.4. Validation

Our numerical results are validated against the experimental work carried out by Parsazadeh [50]. A PCM (coconut oil) melting behavior in a 60 × 60 mm square enclosure is investigated. The enclosure is heated isothermally at the bottom, and the rest of the walls are insulated. The initial temperature of the square enclosure is at 15 °C, and a constant heated wall temperature of 55 °C is specified. The liquid fraction percentage is plotted against time in Fig. 4 (a), and fine accordance between numerical and experimental results is observed. An average deviation of 4.56 % is spotted between experimental and numerical simulations. The average deviation was calculated based on the difference between the average value reported in the literature and the current study to the average value reported in the literature.

When using multiple PCMs, our results were compared with those obtained by [37], which used three different PCMs, RT-55, RT-60, and RT-65. At the initial temperature of 353 K, a shell and tube heat exchanger was simulated, with an adiabatic boundary condition at the shell side. In Fig. 4 (b), a 3.2 % of average deviation is observed when the liquid fraction is plotted against time.

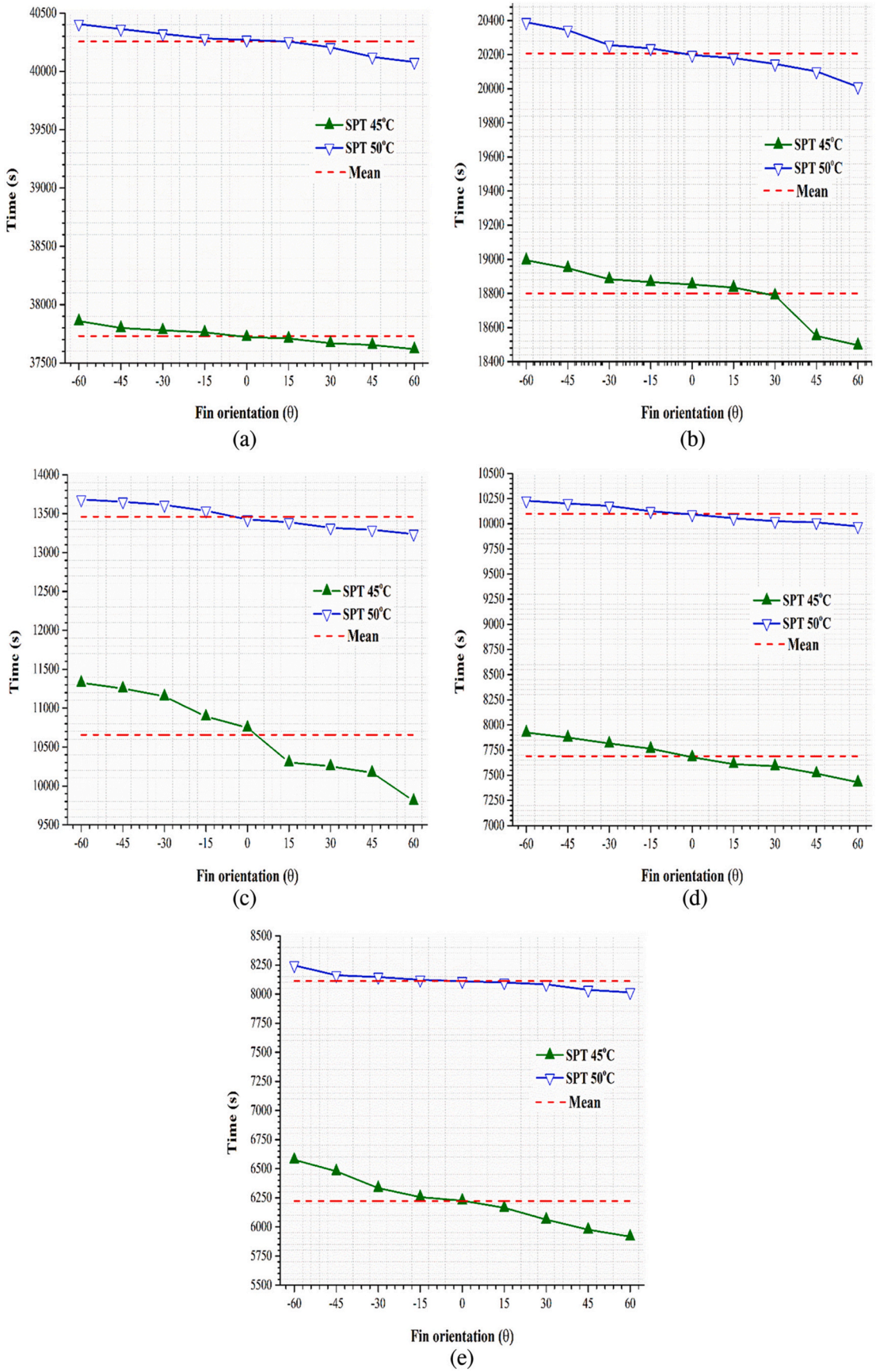

Fig. 9. For varying heat flux time to reach SPT of 45 °C and 50 °C. (a) 100 W/m^2, (b) 200 W/m^2, (c) 300 W/m^2, (d) 400 W/m^2, and (e) 500 W/m^2.

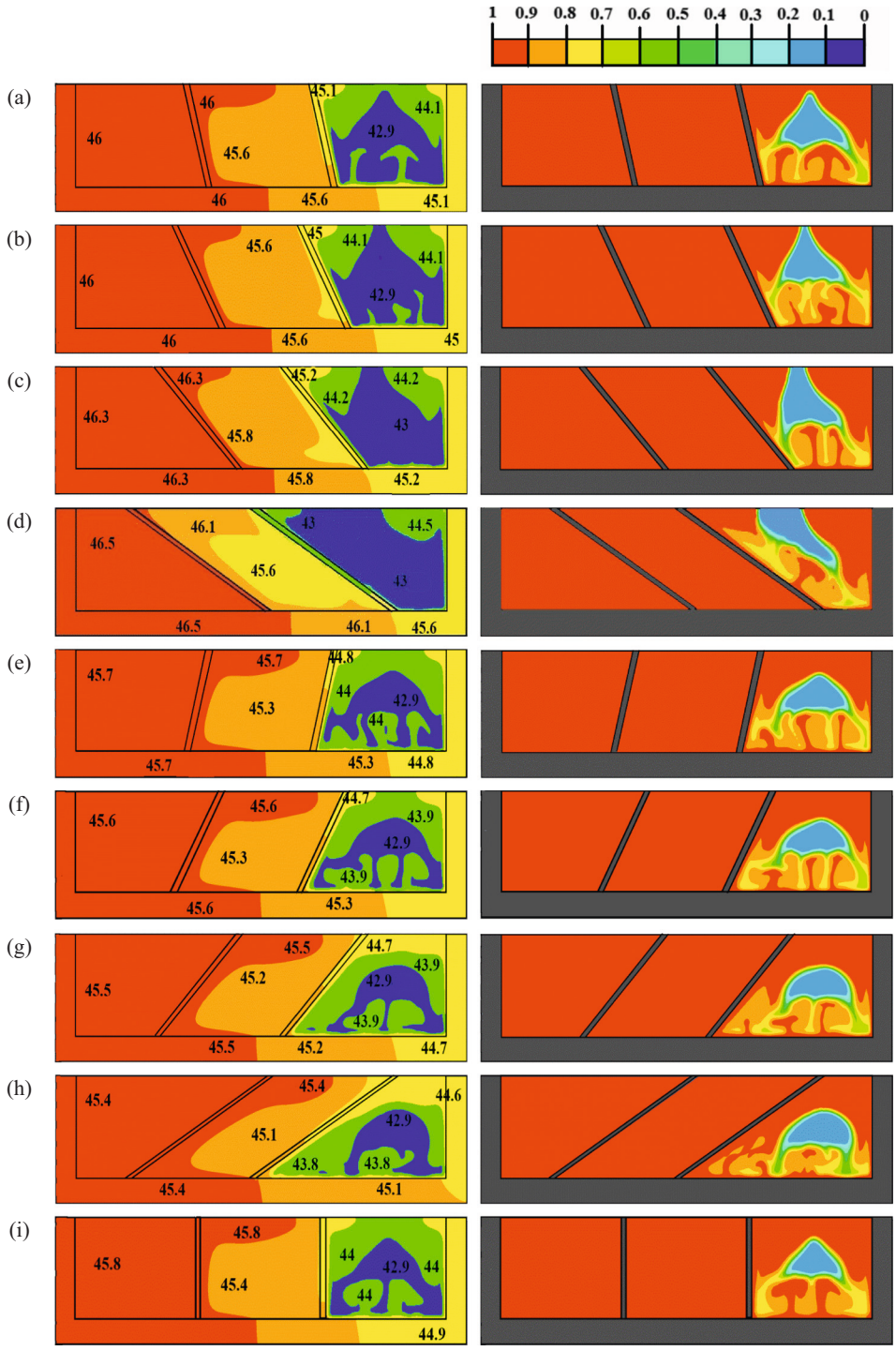

Fig. 10. Contours of temperature distribution and mass fraction at 12000 s (a) +15° (b) +30° (c) +45° (d) +60° (e) -15° (f) -30° (g) -45° (h) -60° (i) 0°.

2.5. *Influence of different arrangement*

As shown in Table 2, six different cases are considered with straight fins in order to determine the best PCM arrangement.

An investigation was conducted to evaluate the effects of different arrangements on a multi-PCM heat sink operating at 500 W/m^2. The average heater temperature of a heat sink is taken and plotted against time in Fig. 5 (a). As seen, the cases studied here lead to indistinguishable wall temperature. Moreover, the time taken for the heater to reach a set point temperature (SPT) of 45 °C and 50 °C is plotted in Fig. 5 (b). The total time required to attain those temperatures is almost the same for all the cases. The time difference between all the cases is found to be 15–20 s. Hence, as demonstrated by Fig. 5 (a), (b), the PCMs can be arranged in any order, in parallel compartments for this basal heating problem.

3. Results and discussion

3.1. *Significance of multiple PCM*

The better performance of the multiple PCM is indicated in Fig. 6. A heat sink with a straight fin is selected for this comparison. Four

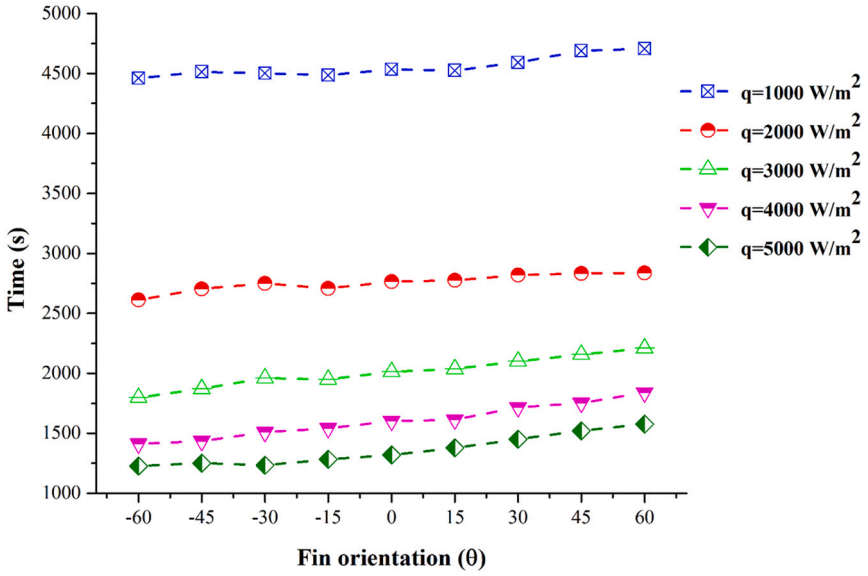

Fig. 11. Completion of charging cycle duration for various fin orientations.

different sinks are investigated: three of them with single-PCM, RT-28HC, RT-35HC, or RT-44HC, and a triple PCM that all three fill the enclosure. A uniform heat flux of 500 W/m^2 is specified at the bottom of the sink. A charging cycle should have extended duration of melting and the discharging cycle must have reduced duration of solidification for an effective heat sink [51]. Hence, numerical simulation has been performed for comparing RT-28 HC PCM heat sink and multiple PCM during solidification. The boundary condition of the heater is specified as ambient temperature and the PCM is at liquid state with 323 K as initial condition. In Fig. 6(c), the solidification time taken for the multiple PCM is 7000 s faster than the heat sink filled with RT-28HC. The latent heat is higher for RT-28HC, hence during charging cycle it helps in prolonged melting but during discharging cycle it increases the time to solidify.

Hence, for charging cycle a different PCM and for discharging cycle a different PCM cannot be selected. Therefore, for both cycles a similar PCM unit must be selected. The incorporation of PCM in a heat sink should account longer charging cycle and shortened discharging cycle. To account longer melting, shorter solidification and transient heat loads, multiple PCM can be suitable for better performance than other cases. Therefore, in this study for melting cases, multiple PCM is selected.

Next, an investigation on a double-PCM design for the different cases is listed below in Table 3.

The evolution of liquid fraction for different cases with double PCM for 500 W/m^2 and 3000 W/m^2 heat flux is shown in Fig. 7. Case E' provides a more extended melting period for both the heat fluxes than other cases. It is due to the combined effect of the properties of RT-28HC and RT-44HC. RT-28 possesses longer latent heat, and it is incorporated in both sides, which increases the latent heat period. Then, RT-44HC, which contains a higher melting temperature, where the heat sink takes a long time to attain this temperature. So, the combined effect of these properties provides a longer duration of the charging cycle.

For a better understanding, all the cases are compared to multiple PCM-based enclosures. For all the double cases, the time duration to complete the charging cycle of double PCM is compared with multiple PCM. In Fig. 8, the "time difference" between the double PCM cases and the triple PCM case is shown. As seen, the time difference is the shortest with case E' because of the favorable thermophysical properties. Next, case C′ indicates a lesser time difference; the outer area is filled with RT-28HC. Due to its higher latent heat, the time taken also increases. Whereas case D′ displays a lesser period than the other cases. Here, the reason seems to be the combined effect of RT-35HC and RT-44HC. This combined case provides a faster melting rate because the difference in melting temperature of both the PCM is lesser and low latent heat compared with others.

3.2. Cases with different heat fluxes

At the bottom of the sink, the average heater temperature against varying heat fluxes 100–500 W/m^2 is presented for different tilted angles. The PCM mass remains the same throughout all cases for all these comparisons. It is observed that because of the insertion of 3 different PCMs, there are three latent heat zones and four sensible heat zones. This latent heat zone depends upon the latent heat of the material, and here latent heat of three PCM are almost similar. So, it is noticed that for all heat fluxes, this zone remains identical. As the heat fluxes increase, the latent heat zone decreases proportionally. All the cases show similar trends. Hence, to distinguish the difference between them, the period for each heat sink case to reach 45 °C and 50 °C is plotted. The mean value is plotted in the figure to observe the difference between the fin orientations. The difference from the mean value gives a clear visualization that there are some significant changes in the time intervals.

Fig. 9 displays the time required for the heat sinks to reach 45 °C and 50 °C for 100–500 W/m^2. It is noted from the figure that +60° is quicker to reach 45 °C and 50 °C than other cases, and -60° is slower to attain this temperature. The reason behind this is, in the positive orientation of fins, the amount of PCM in the RT-28HC zone exposes more to the heater surface and melts quicker than the negative cases. Hence, it is faster to reach the SPT. Likewise, reaching SPT is longer for negative orientation, but melting is faster for negative cases. It is because, at a later period, RT-44HC exposed to the bottom of the heater is more and hence higher heat transfer because of natural convection. Though the positive orientation reaches quicker to SPT, the completion of melting takes longer because the RT-44HC zone exposed to the heater is small. Since a lesser amount is exposed to the heater, the PCM present at the top side takes longer to melt. The contours of temperature distribution within the enclosure and mass fraction of multiple PCMs are displayed in Fig. 10 to have a clear visualization. For increasing angle, the unmelted zone expands with positive fin orientation, and with negative fin orientation, the unmelted area shrinks at the RT-44HC spot. The reason is the natural convection dominance at higher angles at negative orientation and more high melting temperature zone exposed to the heater. The melting rate is

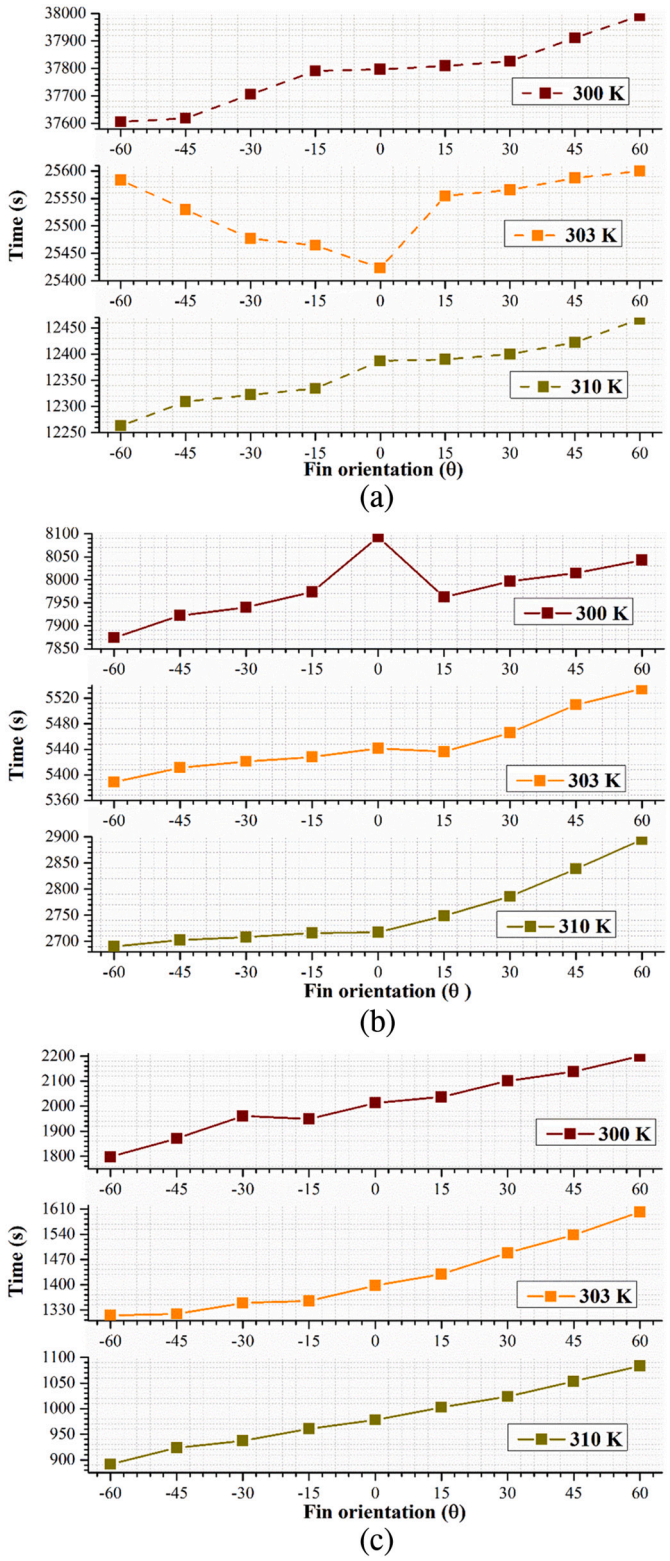

Fig. 12. Time duration for completion of melting at different initial conditions at (a) 100 W/m^2, (b) 500 W/m^2, and (c) 3000 W/m^2.

expedited at a high melting temperature PCM/RT-44HC zone for negative orientation.

The heat fluxes are further increased from 1000 to 5000 W/m^2 to monitor the effect of orientation of fins at higher inputs. The time required for complete melting diminishes with increasing heat flux. As the heat flux increases, the latent heat zone reduces further. As mentioned before, the latent heat zone, which is seen at lower heat fluxes, is absent at higher flux. The time taken for the completion of charging cycles for higher heat flux is presented in Fig. 11. Compared with straight fins (0°), the positive angle tilted fins show an extended melting time. It is easily understood that when the fins are oriented towards the left side of the enclosure (+ve), melting is delayed. This is because of the amount of higher melting temperature PCM remaining at the end, and when angles are increased, completion of melting is retarded. Considering the negative orientation of fins, melting time is lesser than the straight fin. For all varying heat flux, −60° orientation yields a shortened melting rate since the heater is at the bottom of the enclosure; the high melting temperature PCM (RT-44HC) is mainly exposed to the heater and sidewalls of the enclosure. Thus, less part at the top of the heater melts earlier for this case due to gravity. These phenomena are observed for both low and high heat flux.

3.3. Cases with different initial conditions

As the initial temperature is varied, the state of PCM inside the enclosure also varies. Here the initial temperatures included for the study are 300 K, 303 K, and 310 K. For 300 K, all three PCMs are solid-state. With 303 K as the initial condition, RT-28HC is in the liquid state, and RT-35HC and RT-44HC are solid. Simultaneously, for 310 K, RT-28 and RT-35HC are liquid, and RT-44HC is solid-state. For low (100 and 500 W/m^2) and high (3000 W/m^2) heat flux, the duration of completion of melting is given for different initial conditions in Fig. 12.

For any heat flux, at 300 K and 310 K initial condition, the time taken for the charging cycle to complete is longer for positive orientation and shorter for negative orientation. At 300 K, all three PCMs are at solid-state. As discussed earlier, for the 300 K initial condition, the melting rate is higher for positive orientation at the initial period. Still, at the later melting period, negative orientation accelerates the melting. Hence, positive orientation of fins shows prolonged melting. At initial condition 310 K, only RT-44HC is in the solid-state; at this state, the RT-44HC near the bottom is more for negative orientation and less for positive orientation. With natural convection, the lesser amount in the top side of the enclosure melts faster for negative orientation. Inversely, for positive orientation, the top side of the enclosure contains more PCM. Though the convection influences the melting, it provides a longer charging cycle.

Similarly, for 303 K, RT-35HC and RT-44HC are in solid-state. For 500 W/m^2 and 3000 W/m^2 positive orientation provides longer melting, and negative orientation shows a shorter melting period. However, at 100 W/m^2, it is found that the negative orientation also displays a slower melting rate compared to straight fins. Possibly, at this point, the natural convection domination for tilted fins is less pronounced. The heat required to melt the PCM for angled fins is insufficient at this heat flux compared with straight fins.

The enhancement percentage for all orientations compared with straight fins is deduced from Eq. (9). For any initial conditions, t_{θ_i} is a total melting time of PCM for respective angled fins and t_{st_i} is the total PCM melting time of straight fin case. The orientation of fins and how it influences melting at different initial conditions is governed by this factor.

$$\text{Enhancement}\% = \frac{t_{st_i} - t_{\theta_i}}{t_{st_i}} \times 100 \tag{9}$$

In Fig. 13, the enhancement percentage for a different initial condition with varying heat flux is displayed. The negative enhancement % states that the corresponding case's total melting time lags with straight fin (0°) total melting time. At 303 K initial condition, when the heat flux is 100 W/m^2 almost for both positive and negative cases, enhancement % is lagging. As mentioned above, at this low heat flux, a straight fin provides superior melting. For all heat inputs and at many conditions, −60° tilted fins have a higher enhancement percentage than the remaining cases. Inversely, the least enhancement percentage is found at

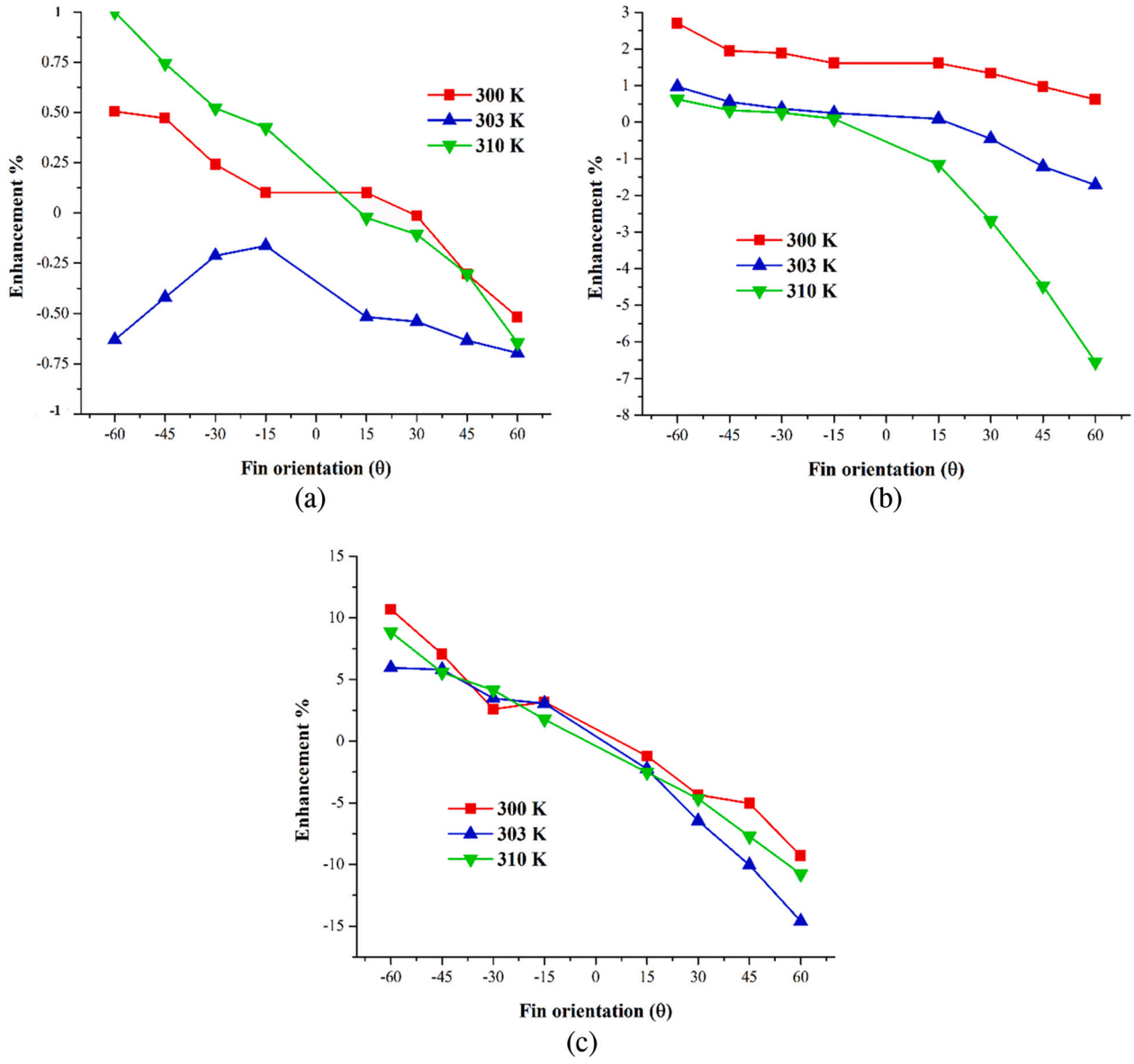

Fig. 13. Enhancement percentage of tilted fins at different initial conditions for (a) 100 W/m^2, (b) 500 W/m^2, and (c) 3000 W/m^2.

60°. It is also perceived that at a higher heat flux of 3000 W/m^2, the enhancement percentage for both orientations escalate for all initial conditions. Other than 303 K at 100 W/m^2, the negative orientation fins exhibit positive enhancement showing a better melting rate than straight fins. Similarly, for positive orientation, other than the 300 K initial condition at 500 W/m^2, the enhancement percentage is negative for all cases. From the plots of the positive orientation fins, it is observed that the duration of the charging cycle is higher than the straight fin.

After these discussions, when employing a triple PCM heat sink with longitudinal fins, the fins can be oriented either way, depending on the scenarios. When prolonged charging cycle is required, positively oriented fins are suitable. The observation states that fins oriented towards the low melting temperature PCM zone for a longer charging cycle are preferred. For rapid melting, -60^0 angled fins, i.e., oriented towards the high melting temperature zone, can be selected. The enhancement percentage is larger with 3000 W/m^2 heat flux at initial conditions. Compared with single and double PCM-based heat sinks, multiple PCM exhibits prolonged melting. For the double PCM heat sink cases, the enclosure contains RT-28HC on both sides, providing extended melting than other double PCM cases.

4. Conclusion

A 2-D rectangular enclosure with multiple PCM is considered for the numerical study. Three different PCM RT-28HC, RT-35HC, and RT-44HC with similar properties are selected and incorporated. Two fins with the same thickness are employed and act as a thermal spreader. In this study, the effects of fin orientation from +60° to -60° are analyzed for charging cycles. The positive and negative orientations are defined by keeping straight fin as a reference. Fins tilted to the left side of straight fins are positive, and tilted towards the right are negative fin orientation. The initial conditions like initial temperature and the initial state of PCM are varied and investigated. A transient model based on the enthalpy-porosity technique was solved using ANSYS fluent 19. The results obtained conclude that,

- The arrangement of multiple PCM in the enclosure does not have a significant effect on the melting period. For 500 W/m^2, the average heater temperature plotted against time intervals displays a similar trend. The time required to attain the SPT of 45 °C and 50 °C also has an inconsiderable deviation between all cases.

- This study compared a single PCM heat sink to multiple PCM heat sinks. Only one PCM is filled in a single PCM enclosure in the entire area. The liquid fraction plotted shows; the multiple PCM enclosures manifest prolonged melting.
- Using a double PCM heat sink, we further explored the significance of multiple PCMs. Two PCM were filled inside each sink to analyze six different cases. RT-28HC filled on both sides of the enclosure, possess extended melting than any other cases. The reason is RT-28HC possesses higher latent heat than other PCM.
- In the case of varying heat fluxes, the negative fin orientation enhances the melting rate compared to the positive orientation of fins. Though the positive orientation fins initially attain SPT of 45 °C and 50 °C quicker, melting completion is delayed. The reason is due to high melting temperature PCM expose towards the bottom wall, and the enclosure heater is very less for positive orientation of fins. Conclusively, −60° and +60° have shortened melting and extended melting, respectively, for low and high heat fluxes.
- The initial temperature of the enclosure is varied by 300 K, 303 K, and 310 K. Simultaneously, the state of the PCM is altered. The enhancement % is found for different heat fluxes, and the effect of this factor is stated. For an initial temperature of 303 K at 100 W/m^2, enhancement % is negative for any cases. At remaining conditions and at different heat fluxes, −60° has a higher enhancement, and + 60° possesses a lower enhancement.

Authors [52–54] have used low heat flux in their study for storing energy in different applications. In most of the cases, with the addition of different enhancers, the weight and cost of the enclosures increase. But, insertion of different PCM to an enclosure instead of machined fins or foams can reduce the manufacturing cost and sink weight. Furthermore, when the density of enhancers increases, the amount of PCM is reduced. This, in turn, reduces the storage capacity of a PCM-based heat sink. In this study, the enclosure size is compact, and when the size of the enclosure increases, the volume of the PCM also increases. Then the enhancement in melting for all angled fin cases also varies. In recent years, electronic devices have almost been mobile. When mobility becomes a major factor, the heat sink can be in any direction. So, accounting for this factor into a PCM-based heat sink, the enhancer orientations also play a major role. This small deviation of angles in the enclosure can lead to a preferable effect.

Moreover, this investigation is an initial study on the multiple PCM-based heat sink on electronic cooling. So, the combination of the fin with multiple PCM has been investigated. These results will be the guidelines for the upcoming study, where the number of PCM can be increased. Therefore, our main concern is employing multiple PCM for thermal management and obtaining their significance in this present work. Also, fins are placed vertically in the heat sink to enhance PCM thermal conductance. In the upcoming study, the effect of fin position, the height of the module, the fin density, and increasing the number of PCM in the heat sink will be considered.

Declaration of competing interest

The authors declare that they have no known competing financial interests or personal relationships that could have appeared to influence the work reported in this paper.

Data availability

Data will be made available on request.

Acknowledgements

Science and Engineering Research Board (SERB), DST No: EEQ/2018/000322, India

References

[1] N. Beemkumar, D. Yuvarajan, M. Arulprakasajothi, S. Ganesan, K. Elangovan, G. Senthilkumar, Experimental investigation and numerical modeling of room temperature control in buildings by the implementation of phase change material in the roof, J. Sol. Energy Eng. Trans. ASME 142 (2020) 1–7, https://doi.org/10.1115/1.4044564.
[2] R. Saxena, N. Agarwal, D. Rakshit, S.C. Kaushik, Suitability assessment and experimental characterization of phase change materials for energy conservation in indian buildings, J. Sol. Energy Eng. Trans. ASME 142 (2020) 1–11, https://doi.org/10.1115/1.4044568.
[3] V. Sun, A. Asanakham, T. Deethayat, T. Kiatsiriroat, Increase of power generation from solar cell module by controlling its module temperature with phase change material, J. Mech. Sci. Technol. 34 (2020) 2609–2618, https://doi.org/10.1007/s12206-020-0336-8.
[4] M. Opolot, C. Zhao, M. Liu, S. Mancin, F. Bruno, K. Hooman, Investigation of the effect of thermal resistance on the performance of phase change materials, Int. J. Therm. Sci. 164 (2021), 106852, https://doi.org/10.1016/j.ijthermalsci.2021.106852.
[5] M. Opolot, C. Zhao, M. Liu, S. Mancin, F. Bruno, K. Hooman, Influence of cascaded graphite foams on thermal performance of high temperature phase change material storage systems, Appl. Therm. Eng. 180 (2020), 115618, https://doi.org/10.1016/j.applthermaleng.2020.115618.
[6] C. Zhao, M. Opolot, M. Liu, F. Bruno, S. Mancin, R. Flewell-Smith, K. Hooman, Simulations of melting performance enhancement for a PCM embedded in metal periodic structures, Int. J. Heat Mass Transf. 168 (2021), https://doi.org/10.1016/j.ijheatmasstransfer.2020.120853.
[7] N. Abdollahi, M. Rahimi, Using a novel phase change material-based cooling tower for a photovoltaic module cooling, J. Sol. Energy Eng. Trans. ASME 142 (2020) 1–6, https://doi.org/10.1115/1.4044890.
[8] B. Ding, Z.H. Qi, C.S. Mao, L. Gong, X.L. Liu, Numerical investigation on cooling performance of PCM/cooling plate hybrid system for power battery with variable discharging conditions, J. Therm. Anal. Calorim. 141 (2020) 625–633, https://doi.org/10.1007/s10973-020-09611-0.
[9] M.M. Heyhat, S. Mousavi, M. Siavashi, Battery thermal management with thermal energy storage composites of PCM, metal foam, fin and nanoparticle, J. Energy Storage. 28 (2020), 101235, https://doi.org/10.1016/j.est.2020.101235.
[10] B. Nie, Z. Du, B. Zou, Y. Li, Y. Ding, Performance enhancement of a phase-change-material based thermal energy storage device for air-conditioning applications, Energy Build. 214 (2020), 109895, https://doi.org/10.1016/j.enbuild.2020.109895.
[11] B. Nie, X. She, Z. Du, C. Xie, Y. Li, Z. He, Y. Ding, System performance and economic assessment of a thermal energy storage based air-conditioning unit for transport applications, Appl. Energy 251 (2019), 113254, https://doi.org/10.1016/j.apenergy.2019.05.057.
[12] M. Joseph, V. Sajith, Graphene enhanced paraffin nanocomposite based hybrid cooling system for thermal management of electronics, Appl. Therm. Eng. 163 (2019), 114342, https://doi.org/10.1016/j.applthermaleng.2019.114342.
[13] R. Du, W. Li, T. Xiong, X. Yang, Y. Wang, K.W. Shah, Numerical investigation on the melting of nanoparticle-enhanced PCM in latent heat energy storage unit with spiral coil heat exchanger, Build. Simul. 12 (2019) 869–879, https://doi.org/10.1007/s12273-019-0527-3.
[14] S. Srinivasan, M.S. Diallo, S.K. Saha, O.A. Abass, A. Sharma, G. Balasubramanian, Effect of temperature and graphite particle fillers on thermal conductivity and viscosity of phase change material n-eicosane, Int. J. Heat Mass Transf. 114 (2017) 318–323, https://doi.org/10.1016/j.ijheatmasstransfer.2017.06.081.
[15] L. Gao, J. Gegentana, B. Bai, D. Sun, S. Che, Li, parametric analysis of a packed bed thermal storage device with phase change material capsules in a solar heating system application, Build. Simul. 14 (2021) 523–533, https://doi.org/10.1007/s12273-020-0686-2.
[16] W. Su, J. Darkwa, G. Kokogiannakis, Numerical thermal evaluation of laminated binary microencapsulated phase change material drywall systems, Build. Simul. 13 (2020) 89–98, https://doi.org/10.1007/s12273-019-0563-z.
[17] S. Mahmoud, A. Tang, C. Toh, R. Al-Dadah, S.L. Soo, Experimental investigation of inserts configurations and PCM type on the thermal performance of PCM based heat sinks, Appl. Energy. 112 (2013) 1349–1356, https://doi.org/10.1016/j.apenergy.2013.04.059.
[18] G.K. Marri, R. Srikanth, C. Balaji, Effect of phase change and ambient temperatures on the thermal performance of a solid-liquid phase change material based heat sinks, J. Energy Storage. 30 (2020), 101327, https://doi.org/10.1016/j.est.2020.101327.
[19] C. Ji, Z. Qin, Z. Low, S. Dubey, F.H. Choo, F. Duan, Non-uniform heat transfer suppression to enhance PCM melting by angled fins, Appl. Therm. Eng. 129 (2018) 269–279, https://doi.org/10.1016/j.applthermaleng.2017.10.030.
[20] X. Yang, X. Wang, Z. Liu, Z. Guo, K. Hooman, Thermal performance assessment of a thermal energy storage tank: effect of aspect ratio and tilted angle, Int. J. Energy Res. 45 (2021) 11157–11178, https://doi.org/10.1002/er.6598.
[21] J.M. Mahdi, S. Lohrasbi, D.D. Ganji, E.C. Nsofor, Simultaneous energy storage and recovery in the triplex-tube heat exchanger with PCM, copper fins and Al2O3 nanoparticles, Energy Convers. Manag. 180 (2019) 949–961, https://doi.org/10.1016/j.enconman.2018.11.038.
[22] A.N. Desai, H. Shah, V.K. Singh, Novel inverted fin configurations for enhancing the thermal performance of PCM based thermal control unit: a numerical study, Appl. Therm. Eng. 195 (2021), 117155, https://doi.org/10.1016/j.applthermaleng.2021.117155.

[23] C. Ji, Z. Qin, S. Dubey, F.H. Choo, F. Duan, Simulation on PCM melting enhancement with double-fin length arrangements in a rectangular enclosure induced by natural convection, Int. J. Heat Mass Transf. 127 (2018) 255–265, https://doi.org/10.1016/j.ijheatmasstransfer.2018.07.118.
[24] A. Arshad, M. Ibrahim Alabdullatif, M. Jabbal, Y. Yan, Towards the thermal management of electronic devices: a parametric investigation of finned heat sink filled with PCM, Int. Commun. Heat Mass Transf. 129 (2021), 105643, https://doi.org/10.1016/j.icheatmasstransfer.2021.105643.
[25] L. Kasper, D. Pernsteiner, M. Koller, A. Schirrer, S. Jakubek, R. Hofmann, Numerical studies on the influence of natural convection under inclination on optimal aluminium proportions and fin spacings in a rectangular aluminium finned latent-heat thermal energy storage, Appl. Therm. Eng. 190 (2021), https://doi.org/10.1016/j.applthermaleng.2020.116448.
[26] J.M. Mahdi, E.C. Nsofor, Multiple-segment metal foam application in the shell-and-tube PCM thermal energy storage system, J. Energy Storage. 20 (2018) 529–541, https://doi.org/10.1016/j.est.2018.09.021.
[27] Z.Q. Zhu, Y.K. Huang, N. Hu, Y. Zeng, L.W. Fan, Transient performance of a PCM-based heat sink with a partially filled metal foam: effects of the filling height ratio, Appl. Therm. Eng. 128 (2018) 966–972, https://doi.org/10.1016/j.applthermaleng.2017.09.047.
[28] C. Zhao, M. Opolot, M. Liu, F. Bruno, S. Mancin, K. Hooman, Phase change behaviour study of PCM tanks partially filled with graphite foam, Appl. Therm. Eng. 196 (2021), 117313, https://doi.org/10.1016/j.applthermaleng.2021.117313.
[29] B.V.S. Dinesh, A. Bhattacharya, Comparison of energy absorption characteristics of PCM-metal foam systems with different pore size distributions, J. Energy Storage. 28 (2020), 101190, https://doi.org/10.1016/j.est.2019.101190.
[30] H. Zheng, C. Wang, Q. Liu, Z. Tian, X. Fan, Thermal performance of copper foam/paraffin composite phase change material, Energy Convers. Manag. 157 (2018) 372–381, https://doi.org/10.1016/j.enconman.2017.12.023.
[31] S. Mancin, A. Diani, L. Doretti, K. Hooman, L. Rossetto, Experimental analysis of phase change phenomenon of paraffin waxes embedded in copper foams, Int. J. Therm. Sci. 90 (2015) 79–89, https://doi.org/10.1016/j.ijthermalsci.2014.11.023.
[32] X. Cheng, X. Zhai, Thermal performance analysis of a cascaded cold storage unit using multiple PCMs, Energy 143 (2018) 448–457, https://doi.org/10.1016/j.energy.2017.11.009.
[33] L.N. N., Assessment of latent heat thermal storage systems operating with multiple phase change materials, J. Energy Storage 23 (2019) 442–455, https://doi.org/10.1016/j.est.2019.04.008.
[34] O.S. Elsanusi, E.C. Nsofor, Melting of multiple PCMs with different arrangements inside a heat exchanger for energy storage, Appl. Therm. Eng. 185 (2021), 116046, https://doi.org/10.1016/j.applthermaleng.2020.116046.
[35] V.S. Vigneswaran, G. Kumaresan, B.V. Dinakar, K.K. Kamal, R. Velraj, Augmenting the productivity of solar still using multiple PCMs as heat energy storage, J. Energy Storage. 26 (2019), 101019, https://doi.org/10.1016/j.est.2019.101019.
[36] M. Ezra, Y. Kozak, V. Dubovsky, G. Ziskind, Analysis and optimization of melting temperature span for a multiple-PCM latent heat thermal energy storage unit, Appl. Therm. Eng. 93 (2016) 315–329, https://doi.org/10.1016/j.applthermaleng.2015.09.040.
[37] J.M. Mahdi, H.I. Mohammed, E.T. Hashim, P. Talebizadehsardari, E.C. Nsofor, Solidification enhancement with multiple PCMs, cascaded metal foam and nanoparticles in the shell-and-tube energy storage system, Appl. Energy 257 (2020), 113993, https://doi.org/10.1016/j.apenergy.2019.113993.
[38] H. Usman, H.M. Ali, A. Arshad, M.J. Ashraf, S. Khushnood, M.M. Janjua, S.N. Kazi, An experimental study of PCM based finned and un-finned heat sinks for passive cooling of electronics, Heat Mass Transf. Und Stoffuebertragung. 54 (2018) 3587–3598, https://doi.org/10.1007/s00231-018-2389-0.
[39] C.S. Miers, A. Marconnet, Experimental investigation of composite phase change material heat sinks for enhanced passive thermal management, J. Heat Transf. 143 (2021) 10–12, https://doi.org/10.1115/1.4048620.
[40] M.A. Hayat, H.M. Ali, M.M. Janjua, W. Pao, C. Li, M. Alizadeh, Phase change material/heat pipe and copper foam-based heat sinks for thermal management of electronic systems, J. Energy Storage. 32 (2020), 101971, https://doi.org/10.1016/j.est.2020.101971.
[41] A. Arshad, M. Jabbal, P.T. Sardari, M.A. Bashir, H. Faraji, Y. Yan, Transient simulation of finned heat sinks embedded with PCM for electronics cooling, Therm. Sci. Eng. Prog. 18 (2020), 100520, https://doi.org/10.1016/j.tsep.2020.100520.
[42] S.K. Sahoo, M.K. Das, P. Rath, Application of TCE-PCM Based Heat Sinks for Cooling of Electronic Components: A Review, Elsevier, 2016, https://doi.org/10.1016/j.rser.2015.12.238.
[43] K.Y. Leong, S.P. Chew, B.A. Gurunathan, K.Z. Ku Ahmad, H.C. Ong, An experimental approach to investigate thermal performance of paraffin wax and 1-hexadecanol based heat sinks for cooling of electronic system, Int. Commun. Heat Mass Transf. 109 (2019), 104365, https://doi.org/10.1016/j.icheatmasstransfer.2019.104365.
[44] N. Hu, L.W. Fan, Z.Q. Zhu, Can the numerical simulations of melting in a differentially-heated rectangular cavity be rationally reduced to 2D? A comparative study between 2D and 3D simulation results, Int. J. Heat Mass Transf. 166 (2021), 120751, https://doi.org/10.1016/j.ijheatmasstransfer.2020.120751.
[45] T.H. Sherer, Y. Joshi, Numerical and experimental investigation of Shell-and-tube phase-change material thermal energy storage unit, J. Electron. Packag. Trans. ASME 138 (2016) 1–10, https://doi.org/10.1115/1.4034101.
[46] RUBITHERM , (n.d.). https://www.rubitherm.eu/en/.
[47] M. Faden, A. König-Haagen, S. Höhlein, D. Brüggemann, An implicit algorithm for melting and settling of phase change material inside macrocapsules, Int. J. Heat Mass Transf. 117 (2018) 757–767, https://doi.org/10.1016/j.ijheatmasstransfer.2017.10.033.
[48] M. Fadl, P.C. Eames, An experimental investigations of the melting of RT44HC inside a horizontal rectangular test cell subject to uniform wall heat flux, Int. J. Heat Mass Transf. 140 (2019) 731–742, https://doi.org/10.1016/j.ijheatmasstransfer.2019.06.047.
[49] ANSYS Inc , ANSYS Fluent Software Package v19.5, (n.d.). https://www.afs.enea.it/project/neptunius/docs/fluent/html/ug/main_pre.htm.
[50] M. Parsazadeh, X. Duan, Numerical and experimental investigation of phase change heat transfer in the presence of rayleigh-benard convection, J. Heat Transf. 142 (2020) 1–13, https://doi.org/10.1115/1.4046537.
[51] S. Sridharan, R. Srikanth, C. Balaji, Multi objective geometric optimization of phase change material based cylindrical heat sinks with internal stem and radial fins, Therm. Sci. Eng. Prog. 5 (2018) 238–251, https://doi.org/10.1016/j.tsep.2017.10.003.
[52] K. Kant, A. Shukla, A. Sharma, P.H. Biwole, Melting and solidification behaviour of phase change materials with cyclic heating and cooling, J. Energy Storage. 15 (2018) 274–282, https://doi.org/10.1016/j.est.2017.12.005.
[53] S. Huang, J. Lu, Y. Li, L. Xie, L. Yang, Y. Cheng, S. Chen, L. Zeng, W. Li, Y. Zhang, L. Wang, Experimental study on the influence of PCM container height on heat transfer characteristics under constant heat flux condition, Appl. Therm. Eng. 172 (2020), 115159, https://doi.org/10.1016/j.applthermaleng.2020.115159.
[54] M. Mobedi, K. Hooman, W. Tao, Solid-Liquid Thermal Energy Storage: Modeling and Applications, CRC Press, 2022.